Mon. Not. R. Astron. Soc. **000**, 1–9 (2014) Printed 23 June 2014 (MN LATEX style file v2.2)

C IV absorption line variability in X-ray bright BALQSOs

Ravi Joshi [1⋆], Hum Chand [1], Raghunathan Srianand [2], Jhilik Majumdar [3]

[1] *Aryabhatta Research Institute of Observational Sciences (ARIES), Manora Peak, Nainital – 263 002, India*
[2] *Inter-University Centre for Astronomy and Astrophysics (IUCAA), Postbag 4, Ganeshkhind, Pune 411 007, India*
[3] *Jadavpur University, Kolkata 700 032, India*

arXiv:1401.5593v2 [astro-ph.GA] 29 Apr 2014

Accepted —. Received —; in original form —

ABSTRACT

We report kinematic shift and strength variability of C IV broad absorption line (BAL) trough in two high-ionization X-ray bright QSOs SDSS J085551+375752 (at $z_{\rm em} \sim 1.936$) and SDSS J091127+055054 (at $z_{\rm em} \sim 2.793$). Both these QSOs have shown combination of profile shift, appearance and disappearance of absorption components belonging to a single BAL trough. The observed average kinematic shift of whole BAL profile resulted in an average deceleration of $\sim -0.7 \pm 0.1$, -2.0 ± 0.1 cm s^{-2} over a rest-frame time-span of 3.11 yr and 2.34 yr for SDSS J085551+375752 and SDSS J091127+055054, respectively. To our knowledge, these are the largest kinematic shifts exceeding by factor of about 2.8, 7.8 than the highest deceleration reported in the literature; making both of them as a potential candidate to investigate outflows using multi-wavelength monitoring for their line and continuum variability. We explore various possible mechanisms to understand the observed profile variations. Outflow models involving many small self-shielded clouds moving probably in a curved path provides the simplest explanation for the C IV BAL strength and velocity variations along with the X-ray bright nature of these sources.

Key words: galaxies: active - quasars: absorption lines - quasars: general quasars: individual: J085551+375752, J091127+055054.

1 INTRODUCTION

About 10−20 per cent of the QSO population shows strong blueshifted broad absorption lines (henceforth called BALQSOs), with velocity widths greater than 2000 km s^{-1} and typical outflow velocities of 1000−30,000 km s^{-1}(e.g., Weymann et al. 1991). This has been interpreted as a signature of outflows from the accretion disc. Outflows play an important role in controlling the growth of the central massive black hole, the evolution of the host galaxy and the chemical enrichment of the inter-galactic medium (e.g., Ostriker et al. 2010). However, the basic physical conditions, acceleration mechanism(s), location and three dimensional structure of QSO outflows are poorly understood. Line variability study is one of the powerful methods which can provide useful insights into the structure and dynamics of the outflowing gas. In the case of BALQSOs such line variability is commonly reported as changes in the absorption strength (e.g. Hamann et al. 1997; Srianand & Petitjean 2001; Misawa et al. 2005; Lundgren et al. 2007; Hall et al. 2011; Capellupo et al. 2012a,b, 2013; Filiz Ak et al. 2013; Vivek et al. 2014); and/or appearance, disappearance of absorption trough (e.g., Hamann et al. 2008; Rodríguez Hidalgo et al. 2011; Vivek et al. 2012a,b; Hamann et al. 2013). However, the kinematic shift in BAL profiles have also been seen in very few cases (e.g., Vilkoviskij & Irwin 2001; Gabel et al. 2003; Hall et al. 2007). The observed behavior of appearance or disappearance of BAL trough, their absorption strength variation and the kinematic shift in absorption profile are most readily understood as a result of (i) changes in the ionization state as a function of velocity in a fixed outflow; (ii) changes in the acceleration profile and/or geometry of the outflow due to change in the driving force or mass-loss rate; (iii) by actual line of sight acceleration of a shell of material from a continual flow; and, (iv) due to transverse motion of the absorbing cloud(s) relative to the line of sight (Gabel et al. 2003; Hall et al. 2007; Lundgren et al. 2007; Capellupo et al. 2011; Vivek et al. 2012a).

In a general scenario, BAL outflows are believed to arise from the QSO's accretion disc and driven by the radiation pressure (Arav & Li 1994; Murray et al. 1995; Proga et al. 2000; Proga & Kallman 2004). However, the required radi-

⋆ E-mail: ravi@aries.res.in (RJ); hum@aries.res.in (HC); anand@iucaa.ernet.in (RS); jhilik3837@gmail.com (JM)

ation to push the outflow at a high relativistic speed may also over-ionize the gas and hence make it transparent to the radiation that drives the flow. This problem is resolved by proposing the radiative shield only to be close to the base of the outflow (Murray et al. 1995). This has also been used to explain the X-ray weakness of BALQSOs compared to normal QSOs by attributing the X-ray weakness to the absorption due to high H I column densities (N_H) in the range of $10^{22} - 10^{24}$ cm^{-2}, due to radiative shield closer to the disc plane (e.g., Wang et al. 1999; Proga & Kallman 2004; Gallagher et al. 2006; Stalin et al. 2011). However, origin of the X-ray weakness in BALQSOs is a matter of debate until now.

Further, the observations of narrow absorption line outflows ($\sim$ 2000 km s^{-1}, some times refer to as "mini-BALs") have extended the above canonical picture by assigning these mini-BAL outflows to the sight lines at higher latitudes that perhaps skim the edge of main BAL flows farther above the disc (Ganguly et al. 2001; Hamann et al. 2008). This was also supported by the observed weak X-ray absorption in mini-BALs, if the X-ray absorbers resides primarily near the accretion disc as proposed above. Additional complication arises when we consider that mini-BALs also possess the very high-speed and moderate ionization as normal BALs, even without the protection of a radiative shield (Hamann et al. 2013). This might suggest that the shield may not be a critical feature of the wind, and hence, perhaps the models involving continuous flow with radiative shield may need replacement with the models involving many small self shielded clouds with low volume filling factor and driven out by radiative force while being confined by magnetic pressure (de Kool & Begelman 1995; Rees 1987). Such clouds with magnetic confinement are also shown to have super thermal velocity dispersion and therefore only few of them can explain the observed broad and smooth BAL profiles (e.g., see Bottorff & Ferland 2000; Hamann et al. 2013). In such mechanism one would expect mixing of line shift and line strength variability introduced by small multiple clouds in contrast to a smooth variability in models of homogeneous outflows. The observational signatures for such scenarios are still awaited, for which study of the BALQSOs having broad absorption trough (like normal BALs) as well as being X-ray bright in nature (like mini-BALs) will be ideal candidates. Interestingly, such new population of X-ray bright BALQSOs have been discovered in recent X-ray surveys (e.g., Giustini et al. 2008; Gibson et al. 2009; Streblyanska et al. 2010; Stalin et al. 2011). The line-variability study of these sources may provide some useful hints towards understanding of the above issues of outflow kinematics including the key question of BALQSOs being overall X-ray weak (i.e., either intrinsic or absorbed).

Recently, we have started a pilot project for the spectral variability monitoring of 10 high-ionization BALQSOs detected in X-rays from the compilation of Giustini et al. (2008), Gibson et al. (2009) and Streblyanska et al. (2010). This sample has been constructed with the BALQSOs having (i) optical to X-ray spectral index, α_{ox}[1], greater than -1.8; (ii) the SDSS $g_{mag} < 19.0$, to achieve a good signal to noise ratio with 2-m class telescopes, in a reasonable exposure time; and (iii) the redshift range of approximately $1.6 < z < 3.6$, in order to cover the C IV BAL trough in spectral range of 3800 − 6840 Å found most suitable in our observational plan (see below). Among our full sample we found two interesting cases of C IV BAL trough variation, here we present a detailed analysis of these systems. The detail results based on our full sample will be presented elsewhere.

This paper is organized as follows. Section 2 describes our analysis including observations, data reduction and spectral analysis. In Section 3, we present the results of our analysis, followed by a discussion in Section 4 and finally our conclusions in Section 5.

2 ANALYSIS

2.1 Observation and Data Reduction

The observations were carried out using the IFOSC mounted on the 2 meter telescope in IUCAA Girawali Observatory (IGO). We have taken a long-slit spectra covering the wavelength range 3800−6840 Å using Grism[2] #7 of IFOSC with a resolution $R \sim 1140$, to cover the C IV and Si IV lines, respectively. A slit width of either 1.″0 or 1.″5 is used. Typical seeing during our observations were around 1.″2 to 1.″4. The raw CCD frames were cleaned using standard IRAF[3] procedures. The Halogen flats were used for the flat fielding the frames. We then extracted the one dimensional spectrum from individual frames using the IRAF task "apall". Wavelength calibration of the spectra was performed using Helium-Neon lamp. The spectrophotometric flux calibration was done using standard stars and assuming a mean extinction for the IGO site. In cases of multiple exposures we co-added the flux with $1/\sigma_i^2$ weightage, where σ_i is the error on the individual pixel. The error spectrum was computed taking into account proper error propagation during the combining process. The spectrum was corrected to vacuum helio-centric frame.

The reduced one-dimensional spectra of BALQSOs for the comparison were downloaded from the SDSS and SDSS-BOSS Data Archive Server[4]. Details about the SDSS spectral information can be found in York et al. (2000). Briefly, these SDSS spectra cover a spectral range from 3800 to 9200 Å, with a resolution ($\lambda/\Delta\lambda$) of about 2000 (i.e. 150 km s^{-1}). The BOSS spectra have wavelength coverage between 3600 − 10000 Å at a resolution of 1300 − 3000 (see Dawson et al. 2013), as listed in column 5 of Table 1.

2.2 Continuum Fitting

In order to have accurate measurements of variability in absorption lines, one needs to carefully take into account the

[1] Ratio between the monochromatic luminosities L_ν at 2 keV and 2500 Å as, $\alpha_{ox} \equiv 0.3838 \log\left(\frac{L_\nu(2\text{ keV})}{L_\nu(2500\text{ Å})}\right)$

[2] http://www.iucaa.ernet.in/~itp/etc/ETC/help.html#grism

[3] IRAF is distributed by the National Optical Astronomy Observatories, which are operated by the Association of Universities for Research in Astronomy, Inc., under cooperative agreement with the National Science Foundation.

[4] http://data.sdss3.org/bulkSpectra

Table 1. Log of observations and other basic parameters of the spectra.

QSO	Instrument	Date (MJD)	Exposure Time (mins)	Resolution (km s^{-1})	S/N [a]
(1)	(2)	(3)	(4)	(5)	(6)
	SDSS	52643	55×1	150	16
J0855+3757	IGO/IFOSC 7[b]	55568	45×2	310	16
	SDSS-BOSS	55973	60×1	150	23
	SDSS	52650	52×1	150	24
	IGO/IFOSC 7	55568	45×2	310	17
	SDSS-BOSS	55896	60×1	150	26
J0911+0550	IGO/IFOSC 7	55930	45×10[c]	310	48
	IGO/IFOSC 1	55979	45×3	370	15

[a] Signal-to-noise ratio over the wavelength range 5800−6200 Å.
[b] Wavelength coverage of 3800−6840 Å.
[c] Among them 5 exposures belongs to observation taken after two days, i.e., on MJD 55932 .

continuum as well as the emission line fluxes. This is necessary because of uncertainties in the flux calibration and possible real changes in the QSO emission lines. To model the continuum over the spectrum comprising of the broad C IV absorption line region in the rest wavelength range between 1270 and 1800 Å, first we have used a single power law, i.e. $a\lambda^{-\alpha}$, along with a lower (e.g., second) order polynomial, constrained by the measured flux in emission and absorption free regions namely $1323-1338$ Å, $1440-1450$ Å (except for J085551+375752 having absorption) and $1680-1800$ Å in QSOs rest-frame. We use the emission redshift, $z_{\rm em}$, from Hewett & Wild (2010), who have refined the SDSS emission redshift values by reducing the net systematic errors by almost a factor of 20, attaining an accuracy of up to 30 km s^{-1}.

In order to measure the absorption line variability, it is imperative to take into account any emission line flux variation as well. For this we also carry out simultaneous fit[5] of emission lines with multiple Gaussian profiles without associating any physical meaning to them. However, fitting the C IV emission lines has additional complications due to (i) its asymmetric line profile and (ii) the presence of absorption features in the emission line region which makes the estimation of QSO continua highly uncertain. Therefore, first we masked the wavelength regions having absorption signature and then used between one to three Gaussian to define the C IV line profile over the spectra already normalized with our power law fit (see above). All other emission features in the spectrum, such as (i) the iron emission blend redward of the C IV emission line, especially in the range $1500-3500$ Å (e.g., Vanden Berk et al. 2001); (ii) the Si IV emission line and any other feature similar to the emission line profile are modelled with a single Gaussian. Lower panels in Fig. 1 and 2, shows our final continuum fit (the dashed line) comprising of a power law, a lower order polynomial and the multi-Gaussian components, for J085551+375752 and J091127+055054 respectively.

To estimate the spectral variability, the highest signal-to-noise (S/N) ratio BOSS spectrum, is selected as a reference spectrum for comparing with SDSS and IGO spectra. Both the SDSS and BOSS data have similar spectral resolution, however, while comparing two spectra with different resolution such as SDSS/BOSS spectra (i.e., FWHM ~ 2.5 Å) with IGO (i.e., FWHM ~ 4.4 Å) we have degraded the higher resolution spectra to the lower one by using an appropriate Gaussian smoothing. In the following section we provide detailed analysis of the two systems.

[5] To carry out the simultaneous fit we have used the MPFIT package for nonlinear fitting, written in INTERACTIVE DATA LANGUAGE routines. MPFIT is kindly provided by Craig B. Markwardt and is available at http://cow.physics.wisc.edu/~craigm/idl/.

3 RESULTS

3.1 J085551+375752

The optical spectrum of J085551+375752, plotted in Fig. 1, shows a distinct BAL trough of C IV at $z_{\rm abs}\sim$ 1.746, with a BALnicity index (BI, Weymann et al. 1991) of 1296 km s^{-1} (Streblyanska et al. 2010) and an absorption index (AI, Hall et al. 2002) of 1482 km s^{-1} (Trump et al. 2006). However, the corresponding BAL troughs for other high-ionization species such as Si IV and N V are not seen in our spectrum. Its optical to X-ray spectral index, α_{ox}, is found to be -1.78 which is larger than the typical value of soft X-ray weak QSOs having $\alpha_{ox} < -2$ (Giustini et al. 2008).

The pseudo-continuum normalized spectra of J085551+375752 is plotted in upper panel of Fig. 1 in velocity scale, with $v = 0$ km s^{-1} corresponding to reference redshift of, $z_{\rm em} = 1.936$. The plots show the comparisons between the SDSS, IGO and the reference BOSS spectrum over an elapse time of $\Delta t = 9.12$, 1.11 yr in the observed frame, respectively. For visual clarity spectra are smoothed over five pixels. The plot shows that the BAL trough has a striking variation over a velocity range from -29521 to -5670 km s^{-1}, although the change in the equivalent width (EW) is very nominal to be about 18 ± 1 per cent. The quoted error is only the statistical error resulting from the fitting process and does not include any possible systematic error such as from the continuum placement uncertainties.

It can be noted from Fig. 1 that the BAL trough seen in SDSS (MJD 52643) spectrum is composed of one narrow component at ~ -20230 km s^{-1} (marked as $\rm N_{SD}$) and one broad component ranging from -16454 to -8850 km s^{-1} (marked as $\rm B_{SD}$, see Fig. 1). The corresponding components in BOSS/IGO spectrum are subscripted with 'BO', like 'SD', the subscript used to refer the SDSS spectrum. The narrow component in the SDSS spectrum $\rm N_{SD}$ has shown a redward kinematic shift of ~ 675 km s^{-1} as marked $\rm N_{BO}$ in BOSS spectrum. However, the broad component in the SDSS spectrum ($\rm B_{SD}$), has grown in the strength (marked as $\rm B_{BO}$) between the SDSS and IGO (MJD 55568) epoch. Furthermore, no clear signature of deceleration is seen for the narrow component ($\rm N_{SD}$) after the IGO epoch (e.g., see Fig. 1, panel *b*), although a change in the overall absorption strength is noticeable between the IGO (MJD 55568) and BOSS (55973) epoch.

Also it appear that the line profile of $\rm N_{SD}$ component in the SDSS spectrum is nearly similar to the $\rm N_{BO}$ component in the IGO/BOSS spectrum, apart from the above constant velocity shift. This shift along with the likely invariance of line-profile of this component gives a hint of the outflow deceleration, which we have estimated from the position of their line centroid to be $\sim -217.6 \pm 22.2$ km s^{-1}

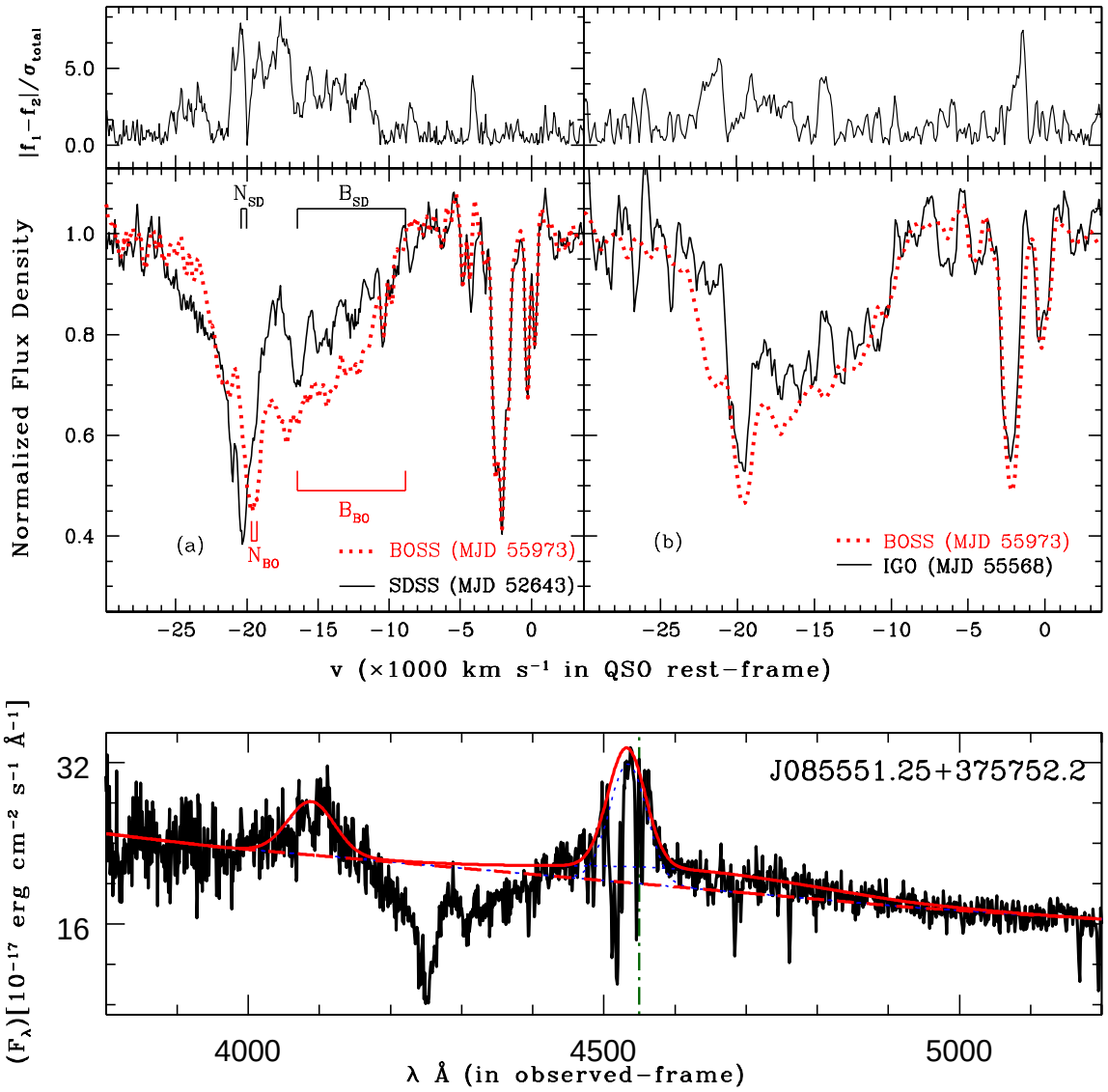

Figure 1. Lower panel: The final continuum fit (smooth curve) comprising of a power law, a lower order polynomial (dashed curve) and the multi-Gaussian components (dotted curve) for SDSS (MJD 52643) spectrum. Middle panel: Two-epoch absorption line variation in a continuum-normalized SDSS, BOSS and IGO spectra for SDSS J085551+375752 in velocity scale, with $v = 0$ km s^{-1} corresponding to QSO emission redshift of $z_{\rm em} = 1.936$. Upper panel: gives the ratio of absolute deviation to the total error-bars.

yr^{-1}(i.e., $\sim -0.7 \pm 0.1$ cm s^{-2}), where for error, a conservative value corresponding to uncertainty of one pixel-shift has been taken.

3.2 J091127+055054

J091127+055054 is a gravitationally lensed QSO at $z_{\rm em} = 2.793$ (Bade et al. 1997). It is also an X-ray bright radio quiet QSO having X-ray luminosity of 4×10^{46} ergs s^{-1} (Bade et al. 1997) and α_{ox} of -1.58 (Giustini et al. 2008). Chandra observations of this source on 1999-11-02 and 2000-10-29, show that its 0.5 − 8.0 keV flux is invariant over the rest-frame time span of about 95 days (Gibson & Brandt 2012). Its optical spectrum shows a distinct BAL trough of C IV at $z_{\rm abs} \sim 2.549$, with a BI value of 2358 km s^{-1} (Streblyanska et al. 2010) and an AI of 1149 km s^{-1} (Trump et al. 2006).

A comparison between SDSS (MJD 52652), IGO (MJD 55568, 55930 and 55979) and the reference BOSS (MJD 55896) spectrum of C IV BAL trough (all smoothed over five pixels), over an observed time span of about 8.89 and 0.89 yr respectively are shown in Fig. 2 in velocity scale with $v = 0$ km s^{-1} corresponding to reference redshift of $z_{\rm em} = 2.793$. From this figure the change and shift in line profile is clearly evident between the SDSS (MJD 52652) and the BOSS (MJD 55896) epoch. Assuming this as a constant velocity shift of the whole profile (e.g., see Fig. 3, where we reproduce the C IV BAL trough spectral portion from

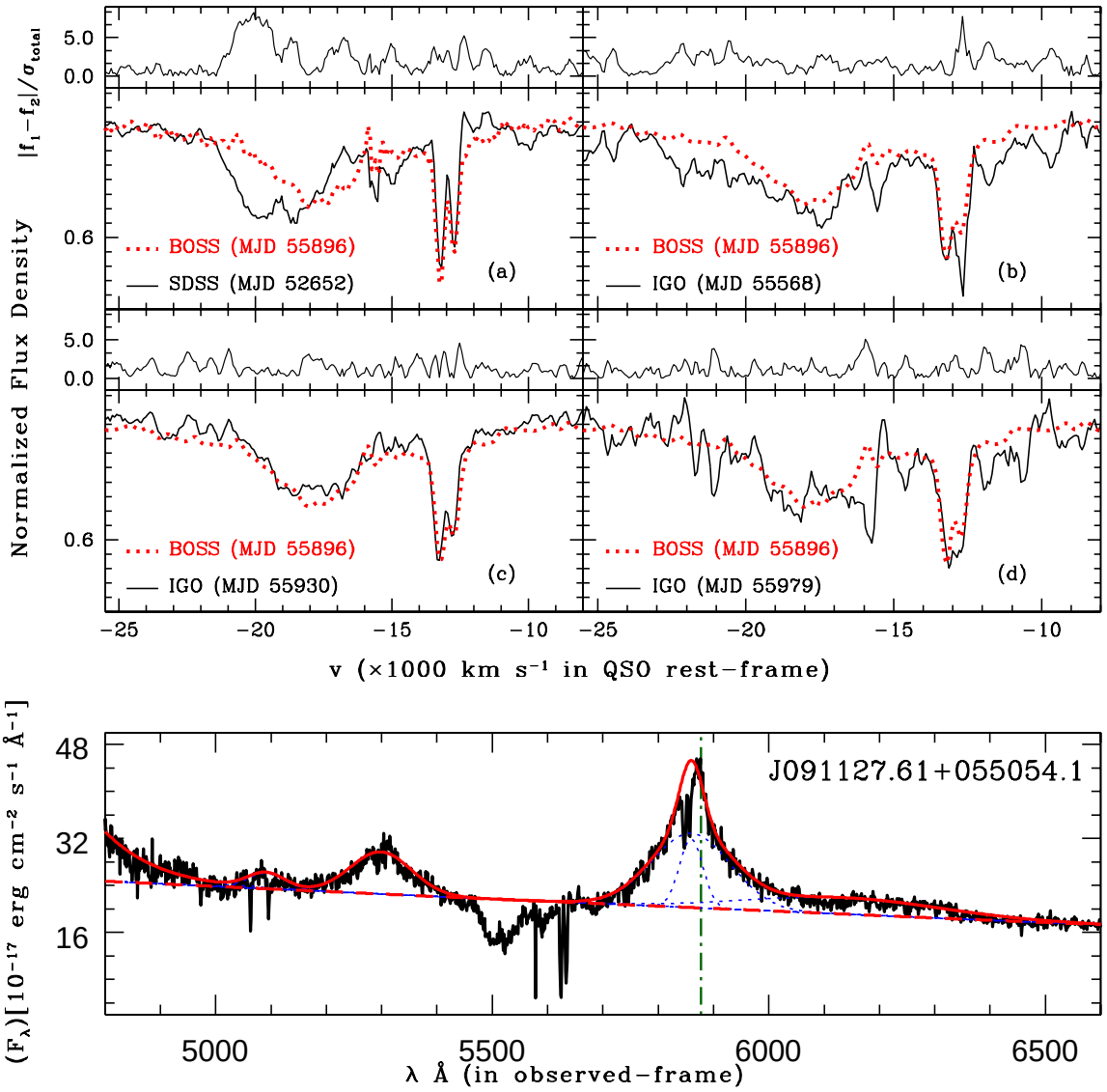

Figure 2. Same as in Figure 1, for the SDSS (MJD 52652) spectrum of SDSS J091127+055054, upper panel: In velocity scales, $v = 0$ km s^{-1} correspond to the QSO emission redshift of $z_{\rm em} = 2.793$.

Fig. 2), one can compute such average shift by using cross-correlation technique by minimizing χ^2 (e.g. see, Hall et al. 2007, and inset in Fig. 4). Using this technique a best-fitting average shift of 21 ± 1 pixel (i.e., ~ 5 Å in QSO rest-frame) has been found between SDSS and BOSS spectrum. It corresponds to a deceleration of $a = -2.0 \pm 0.1$ cm s^{-2}, over a rest-frame time span of 2.34 year. However, no such kinematic shift is noticeable between the BOSS and subsequent IGO spectra (e.g., see Fig. 2).

4 DISCUSSION

In view of the fact that BAL trough variability can be a powerful tool to probe the physical conditions in the vicinity of the QSO, there have been many systematic efforts to detect the EW and the absorption centroid variations (Filiz Ak et al. 2013, and references therein). However, until now very few cases of variability in the absorption kinematics of BAL troughs have been reported (e.g., Vilkoviskij & Irwin 2001; Rupke et al. 2002; Gabel et al. 2003; Hall et al. 2007). A first detection of a change in radial velocity in an outflow associated with a narrow absorption system in a Seyfert 1 galaxy, NGC 3783, is discovered by Gabel et al. (2003), where they found a radial shift in C IV, N V, and Si IV lines. In addition, they also determined a deceleration values of $a = -0.25 \pm 0.05$ and -0.10 ± 0.03 cm s^{-2} over the rest-frame time span of 0.75 and 1.1 yr respectively. Similarly, Hall et al. (2007) have reported the largest BAL trough acceleration in SDSS J024221.87+004912.6 at $a = 0.154 \pm 0.025$ cm s^{-2}over a rest-frame time span of 1.39 yr.

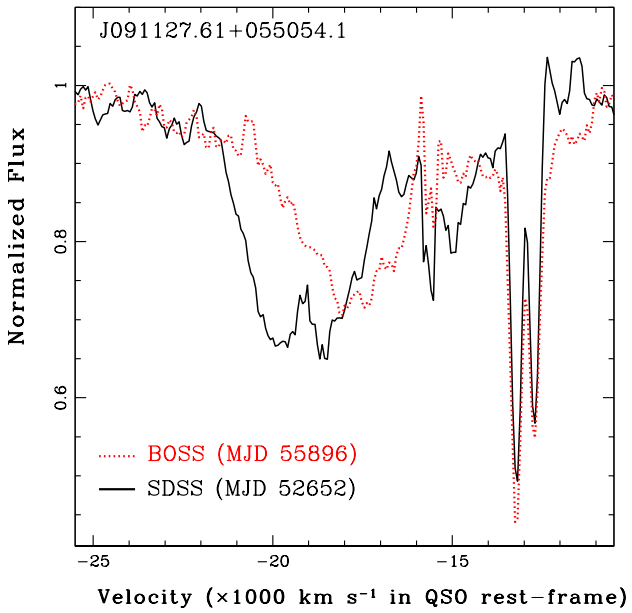

Figure 3. The radial velocity shift observed in J091127.6+055054 for C IV line between SDSS (MJD 52652) (solid thick curve) and BOSS (MJD 55896) epoch (dotted curve) spectrum.

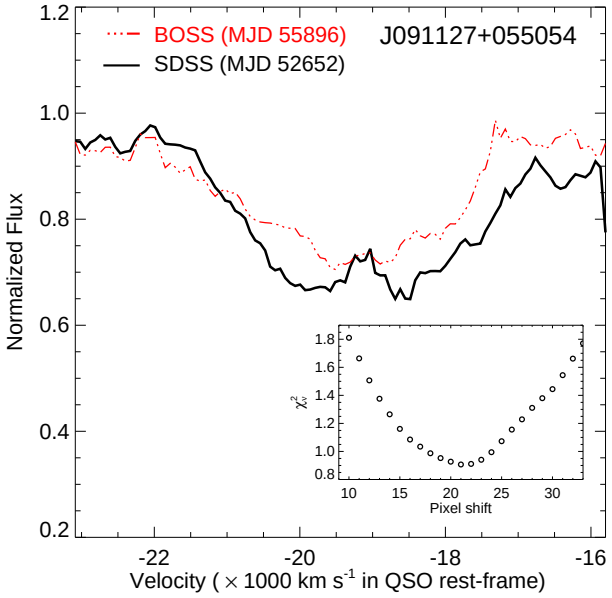

Figure 4. Overplot of SDSS and BOSS epoch spectra for BALQSO J091127.6+055054 after applying best-fitting pixel shift of 21 pixels on BAL trough of BOSS spectrum; the inset displays the χ^2_ν versus pixel shift curve.

Our investigation is related to the BAL variability of less explored X-ray bright BALQSOs, where we have monitored 10 well selected high-ionization X-ray bright BALQSOs (see Section 1). Here, we have reported a discovery of such rarely seen kinematic shift in the C IV BAL trough for two members of our sample, namely J085551+375752 and J091127+055054.

As pointed out in Section 1, some of the main mechanisms proposed to understand such absorption strength and/or kinematic shift in absorption profiles are (i) by actual line-of-sight acceleration/deceleration of a shell of material from a continual flow; (ii) changes in the geometry of the outflow, such as directional shift of outflow; and, (iii) changes in the ionization state as a function of velocity in a fixed outflow. These mechanisms of BAL trough variations are briefly discussed below, as an attempt to constrain the nature of the outflow in our two X-ray bright BALQSOs.

4.1 Deceleration of a continual flow

One possible explanation for the observed decrease in radial velocity is that the absorbing cloud is undergoing a bulk radial deceleration. We first consider gravity as the source of the required inward radial force. The simplest case that the radial force has decreased relative to gravity between the two intervals, can be tested first by estimating the distance of absorbing cloud from the central mass and then carrying out the comparison between outflow speed and the escape velocity at the absorbing cloud location. With an average outflow speed of $\sim$ 20,000 km s^{-1}, absorbing cloud of J085551+375752 and J091127+055054, would have moved by a distance of $\sim 2.1 \times 10^{17}$ cm and $\sim 1.5 \times 10^{17}$ cm, in a rest-frame time span of 3.11, 2.34 yr, respectively, between SDSS and IGO/BOSS epoch. In addition, studies based on photoionization modelling suggests that BAL cloud may be at a distance of several pc to Kpc from the central ionizing source (e.g., see Bautista et al. 2010; Różańska et al. 2014). Hence, assuming a conservative limit of $\sim$ 1 pc for the distance of absorbing cloud from the central ionizing source at the SDSS epoch, the total distance at IGO/BOSS epoch (after including the distance traveled by an outflow since SDSS epoch as estimated above) would be $\sim 3.3 \times 10^{18}$ cm and $\sim 3.2 \times 10^{18}$ cm, for J085551+375752 and J091127+055054 respectively. Given that the central black-hole mass for J085551+375752 and J091127+055054 is about $6.03 \times 10^9 M_\odot$ and $8.31 \times 10^9 M_\odot$, respectively (Shen et al. 2011), we found that the respective escape velocities at the distance of their C IV BAL will be around $\sim$ 6970, $\sim$ 8261 km s^{-1}. Therefore, being both these escape velocities much smaller than the typical observed outflow speed of $\sim 20,000$ km s^{-1}, exclude the possibility of gravitational force being the cause of the deceleration of the outflow and may likely be related to the non-gravitational forces (e.g., see below).

4.2 Directional shift in the outflow

Another simple possibility of the observed decrease in the radial velocity is that the absorbing cloud is moving along a curved path across our line of sight and we are looking at the changing radial component of the velocity vector along our line of sight (e.g., Gabel et al. 2003, see their figure 3). Such curved path trajectories for the BAL outflows are commonly predicted by various mechanisms, such as, the absorber is driven off the accretion disc by the radiation pressure from the central source (Murray et al. 1995; Proga et al. 2000) or by the magneto-hydrodynamic driven winds (e.g. see, Fukumura et al. 2010; Kazanas et al. 2012). For instance,

the magnetically driven disc wind model of Fukumura et al. (2010) predicts the position of C IV ion in winds, which shifts outward along line of sight of decreasing position angle with the disc plane. Further, depending on the observer's inclination, the geometric shape of the magnetic field lines and ionization equilibria may result in the substantial observable change in width/shift of absorption trough, provided clouds motions are curved enough to account for the observed velocity changes (in range of $\sim 217 - 620$ km s^{-1} yr^{-1}). For an observed outflow speed of $\sim 20,000$ km s^{-1}, the predicted inclination angle by Fukumura et al. (2010) is less than 50 degrees and hence for most of the duration while moving along the sight line, absorbing cloud will be covering the background UV continuum source. This avoids the possibility of otherwise changing optical depth also due to probable variation of partial-coverage.

4.3 Photoionization driven BAL variation

In this scenario, the underlying hypothesis is that the unsaturated BAL trough could vary in response to the changing ionization state of QSO central engine, which leads to estimation of the minimum electron density and maximum distance from the continuum source for a photoionized plasma (e.g., Hamann et al. 1997; Hamann 1998; Narayanan et al. 2004).

For J085551+375752, assuming the observed variability time-scale (i.e., 3.11 yr in the QSO rest-frame) as an estimate for recombination time-scale (t_{rec}), then the photoionization equilibrium would imply the electron number density, n_e, to be $\gtrsim 3000$ cm^{-3}(using $n_e \gtrsim [1/(\alpha_r t_{rec})]_{C\ IV}$). Further, the presence of the C IV ions implies that the ionization parameter, U, should be such that $\log U > -2$ (e.g., see Hamann et al. 1997). This in conjunction with the fact that $\log U \propto 1/n_e r^2$ have allowed us to estimate the distance, r, of the absorbing cloud from the QSO centre to be $\lesssim 3$ Kpc.

In addition, no significant continuum variation is found, while comparing SDSS and IGO spectrum (which has better flux calibration than BOSS spectrum). On the other hand, absence of Si IV absorption suggest that the ionization parameter range should be such that when the radiation field increases, the EW of C IV (or its column density) should decrease (e.g., see figure 1 of Hamann et al. 1997) at IGO/BOSS epoch, which indeed is the case as at IGO/BOSS epoch the C IV trough got weakened. So, perhaps, the variability at optical region might be very mild (within uncertainty) but the variability in UV region (that ionizes C IV) may be appreciable, though, more observational constrains will be helpful to conclude firmly about this possibility.

Similarly, for outflow seen in our second source J091127.6+055054, assuming the rest-frame variability time-scale (i.e., 2.34 yr here), as an estimate for recombination time-scale, we have computed the electron number density and the distance of an absorbing cloud from the center of J091127.6+055054 to be $\gtrsim 4000$ cm^{-3} and $\lesssim 5$ Kpc, respectively (using the approach as discussed above for the case of J085551+375752). The continuum flux for this source at 5000 Å has decreased by a factor of about 1.7 between the SDSS and the IGO epoch spectra. Such decrease in the ionizing radiation is also hinted by the C IV emission line that appears stronger (i.e., higher EW due to decrease in continuum) in the IGO/BOSS spectrum than that of earlier epoch SDSS spectrum. We also note here, in Fig. 4, that the overall velocity spread of C IV absorption remains same (apart from shift) between the two epochs, however, the overall absorption strength has weakened. The absorption from other species such as Si IV and N V associated to the C IV BAL trough are not detected in our spectrum. As a result one would expect the allowed ionization parameter range to be such that when radiation field decreases (i.e., dimming of QSO continuum) the absorption line strength of C IV should increase (e.g., see Hamann et al. 1997). In contrast to this, our C IV trough got weakened (e.g., see Fig. 3) with the dimming of our continuum source at IGO/BOSS epoch as compare to SDSS epoch; suggesting that photoionization driven variation mechanism to be unlikely for this case.

In addition to the above discussed scenarios, there are also fair chances for other mechanisms at play as well. For instance, spray of small clouds causing their appearance/disappearance or evolution due to cloud irradiation (e.g., see Proga et al. 2014), along with range of intrinsic velocities, may also result in the observed kinematic shift and strength variability in BAL trough, causing change in resultant optical depth even without variation of flow-speed over time.

5 CONCLUSIONS

In this paper, we present the spectra of two BALQSOs, namely J085551+375752 and J091127+055054, whose broad C IV absorption lines have shown a shift in velocity, between observation spanning a rest-frame time of 3.11 and 2.34 yr, respectively. The shift in the velocity is generally very rare in BALQSOs, and on top of that both these QSOs belong to a rare sub-class of X-ray bright BALQSOs. The X-ray irradiation of any absorbing cloud might play a crucial role in their evolution. For instance, at high X-ray luminosity (L_X) limits, Barai et al. (2012) shows that inner gas will significantly get heat up and expand, which can result into a strong enough outflow capable of expelling most of the gas at larger radii. On the other hand, for some intermediate L_X, thermal instability might even induce a non-spherical feature with cold and dense clumps surrounded by over heated clouds. Similarly, Fan et al. (2009) also found that the BAL properties such as BI and maximum outflow velocities do correlate with the intrinsic X-ray weakness, and suggests that X-ray absorption might probably be necessary for observed BAL outflows.

For our X-ray bright BALQSOs J085551+375752 and J091127+055054, the radial shift we found in our spectrum, resulted in outflow deceleration of about $a = -0.7 \pm 0.1, -2.0 \pm 0.1$ cm s^{-2}, which is about a factor of 2.8 and 7.8 larger than the highest deceleration value reported till now by Gabel et al. (2003) for NGC 3783 with $a = -0.25 \pm 0.05$ cm s^{-2}. We also explore here the main possible mechanisms such as (i) deceleration of a continual flow; (ii) directional shift in the outflow and (iii) the photoionization induced BAL variation, along with other possibility such as, spray of small clouds along the line of sight. We found that the deceleration due to continual flow to be an unlikely mechanism based on our estimation of absorbing

clouds distances from the central mass, where the escape velocity is too small in comparison to the outflow speed (see Section 4.1). The photoionization induced BAL variation may be a possibility for J085551+375752, but seems unlikely for the variation seen in J091127+055054 (e.g., see Section 4.3). On the other hand, the directional shift in the outflow can equally be an explanation for the observed radial shift in both cases, provided the motion is curved enough for observed large velocity shift (about $\sim 217 - 620$ km s^{-1} yr^{-1}). In view of the fact that both of our BALQSOs are X-ray bright, probably their BAL troughs may favor the small clouds scenario, rather than a single homogeneous continuous radial outflow, in conjunction with the scenario of directional shift of outflow motion. However, many small clouds also allow the possibility of other mechanisms such as spray of small clouds causing their appearance/disappearance, with or without curved path motion, can also result in the observed kinematic and/or strength variability in BAL trough, due to the change in optical depth even without variation of speed over time. For the scenario with curved path motion, small clouds close to the disc might contribute, but for scenario with spray of clouds without curve path motion the clouds at higher inclination might be more effective, and hence resultant of them might be responsible for the observed outflow variation seen in our two sources.

We also note that, generally, the effects of covering factor, ionization and optical depth are complexly related, so disentangling these effects would further require the variability follow-ups along with the high-resolution observation as well as a dense sampling of time-variability over larger wavelength coverage, in addition to our present observational constrains. Beside this, as pointed earlier that the majority of line variation do not exhibit velocity shift and these two rare cases which further belong to rare sub-population of X-ray bright BALQSOs, make it difficult to interpret their outflow variation in terms of the global physical properties of BAL outflows. Nonetheless, given the importance of such observed kinematic shift to constrain the possible QSO outflow models, we conclude that J085551+375752 and J091127+055054 are potential candidates to investigate outflow by monitoring them both in optical as well as in X-rays for their lines and/or continuum variability. Also, a systematic search, in large spectroscopic surveys like SDSS/BOSS, for BALQSOs having such kinematic shift and BAL strength variation, will further help to increase the sample of such cases of varying outflows and improve our general understanding of QSO outflows.

ACKNOWLEDGMENTS

We thank an anonymous referee for his/her constructive report to improve our manuscript.

We gratefully acknowledge the observing help rendered by Dr. Vijay Mohan and the observing staff at the IGO 2-m telescope. JM wishes to thank the Indian Academy of Science for their support through Summer Research Fellowship and grateful for hospitality at ARIES.

Funding for the SDSS and SDSS-II has been provided by the Alfred P. Sloan Foundation, the Participating Institutions, the National Science Foundation, the U.S. Department of Energy, the National Aeronautics and Space Administration, the Japanese Monbukagakusho, the Max Planck Society, and the Higher Education Funding Council for England. The SDSS Web Site is http://www.sdss.org/. The SDSS is managed by the Astrophysical Research Consortium for the Participating Institutions. The Participating Institutions are the American Museum of Natural History, Astrophysical Institute Potsdam, University of Basel, University of Cambridge, Case Western Reserve University, University of Chicago, Drexel University, Fermilab, the Institute for Advanced Study, the Japan Participation Group, Johns Hopkins University, the Joint Institute for Nuclear Astrophysics, the Kavli Institute for Particle Astrophysics and Cosmology, the Korean Scientist Group, the Chinese Academy of Sciences (LAMOST), Los Alamos National Laboratory, the Max-Planck-Institute for Astronomy (MPIA), the Max-Planck-Institute for Astrophysics (MPA), New Mexico State University, Ohio State University, University of Pittsburgh, University of Portsmouth, Princeton University, the United States Naval Observatory, and the University of Washington.

REFERENCES

Arav N., Li Z.-Y., 1994, ApJ, 427, 700
Bade N., Siebert J., Lopez S., Voges W., Reimers D., 1997, A&A, 317, L13
Barai P., Proga D., Nagamine K., 2012, MNRAS, 424, 728
Bautista M. A., Dunn J. P., Arav N., Korista K. T., Moe M., Benn C., 2010, ApJ, 713, 25
Bottorff M. C., Ferland G. J., 2000, MNRAS, 316, 103
Capellupo D. M., Hamann F., Shields J. C., Halpern J., Hidalgo P. R., Barlow T. A., 2012a, in Astronomical Society of the Pacific Conference Series, Vol. 460, AGN Winds in Charleston, Chartas G., Hamann F., Leighly K. M., eds., p. 88
Capellupo D. M., Hamann F., Shields J. C., Halpern J. P., Barlow T. A., 2013, MNRAS, 429, 1872
Capellupo D. M., Hamann F., Shields J. C., Rodríguez Hidalgo P., Barlow T. A., 2011, MNRAS, 413, 908
Capellupo D. M., Hamann F., Shields J. C., Rodríguez Hidalgo P., Barlow T. A., 2012b, MNRAS, 422, 3249
Dawson K. S. et al., 2013, AJ, 145, 10
de Kool M., Begelman M. C., 1995, ApJ, 455, 448
Fan L. L., Wang H. Y., Wang T., Wang J., Dong X., Zhang K., Cheng F., 2009, ApJ, 690, 1006
Filiz Ak N. et al., 2013, ApJ, 777, 168
Fukumura K., Kazanas D., Contopoulos I., Behar E., 2010, ApJ, 723, L228
Gabel J. R. et al., 2003, ApJ, 595, 120
Gallagher S. C., Brandt W. N., Chartas G., Priddey R., Garmire G. P., Sambruna R. M., 2006, ApJ, 644, 709
Ganguly R., Bond N. A., Charlton J. C., Eracleous M., Brandt W. N., Churchill C. W., 2001, ApJ, 549, 133
Gibson R. R., Brandt W. N., 2012, ApJ, 746, 54
Gibson R. R. et al., 2009, ApJ, 692, 758
Giustini M., Cappi M., Vignali C., 2008, A&A, 491, 425
Hall P. B. et al., 2002, ApJS, 141, 267
Hall P. B., Anosov K., White R. L., Brandt W. N., Gregg M. D., Gibson R. R., Becker R. H., Schneider D. P., 2011, MNRAS, 411, 2653

Hall P. B., Sadavoy S. I., Hutsemekers D., Everett J. E., Rafiee A., 2007, ApJ, 665, 174
Hamann F., 1998, ApJ, 500, 798
Hamann F., Barlow T. A., Junkkarinen V., 1997, ApJ, 478, 87
Hamann F., Capellupo D., Chartas G., McGraw S., Rodriguez Hidalgo P., Shields J., Charlton J., Eracleous M., 2013, 2013arXiv1302.0201H
Hamann F., Kaplan K. F., Rodríguez Hidalgo P., Prochaska J. X., Herbert-Fort S., 2008, MNRAS, 391, L39
Hewett P. C., Wild V., 2010, MNRAS, 405, 2302
Kazanas D., Fukumura K., Behar E., Contopoulos I., Shrader C., 2012, The Astronomical Review, 7, 030000
Lundgren B. F., Wilhite B. C., Brunner R. J., Hall P. B., Schneider D. P., York D. G., Vanden Berk D. E., Brinkmann J., 2007, ApJ, 656, 73
Misawa T., Eracleous M., Charlton J. C., Tajitsu A., 2005, ApJ, 629, 115
Murray N., Chiang J., Grossman S. A., Voit G. M., 1995, ApJ, 451, 498
Narayanan D., Hamann F., Barlow T., Burbidge E. M., Cohen R. D., Junkkarinen V., Lyons R., 2004, ApJ, 601, 715
Ostriker J. P., Choi E., Ciotti L., Novak G. S., Proga D., 2010, ApJ, 722, 642
Proga D., Jiang Y.-F., Davis S. W., Stone J. M., Smith D., 2014, ApJ, 780, 51
Proga D., Kallman T. R., 2004, ApJ, 616, 688
Proga D., Stone J. M., Kallman T. R., 2000, ApJ, 543, 686
Rees M. J., 1987, QJRAS, 28, 197
Rodríguez Hidalgo P., Hamann F., Hall P., 2011, MNRAS, 411, 247
Różańska A., Nikołajuk M., Czerny B., Dobrzycki A., Hryniewicz K., Bechtold J., Ebeling H., 2014, New A, 28, 70
Rupke D. S., Veilleux S., Sanders D. B., 2002, ApJ, 570, 588
Shen Y. et al., 2011, ApJS, 194, 45
Srianand R., Petitjean P., 2001, A&A, 373, 816
Stalin C. S., Srianand R., Petitjean P., 2011, MNRAS, 413, 1013
Streblyanska A., Barcons X., Carrera F. J., Gil-Merino R., 2010, X-ray Astronomy 2009; Present Status, Multi-Wavelength Approach and Future Perspectives, 1248, 513
Trump J. R. et al., 2006, ApJS, 165, 1
Vanden Berk D. E. et al., 2001, AJ, 122, 549
Vilkoviskij E. Y., Irwin M. J., 2001, MNRAS, 321, 4
Vivek M., Srianand R., Mahabal A., Kuriakose V. C., 2012a, MNRAS, 421, L107
Vivek M., Srianand R., Petitjean P., Mohan V., Mahabal A., Samui S., 2014, MNRAS, 440, 799
Vivek M., Srianand R., Petitjean P., Noterdaeme P., Mohan V., Mahabal A., Kuriakose V. C., 2012b, MNRAS, 423, 2879
Wang T. G., Wang J. X., Brinkmann W., Matsuoka M., 1999, ApJ, 519, L35
Weymann R. J., Morris S. L., Foltz C. B., Hewett P. C., 1991, ApJ, 373, 23
York D. G. et al., 2000, AJ, 120, 1579